Wyss, C. R., Rickenmann, D., Fritschi, B., Turowski, J., Weitbrecht, V., Boes, R. M. (2016): Laboratory flume experiments with the Swiss plate geophone bed load monitoring system: 1. Impulse counts and particle size identification. - *Water Resources Research*, *52*, 10, pp. 7744—7759.

DOI: http://doi.org/10.1002/2015WR018555

AGU PUBLICATIONS

Water Resources Research

RESEARCH ARTICLE
10.1002/2015WR018555

This article is a companion to *Wyss et al.* [2016], doi:10.1002/2016WR019283.

Key Points:
- Systematic flume experiments with the Swiss plate geophone system were performed
- Amplitude and frequency information are combined to identify particle size
- Characteristic signal values of the Swiss plate geophone system are established with flume experiments

Supporting Information:
- Supporting Information S1

Correspondence to:
D. Rickenmann,
dieter.rickenmann@wsl.ch

Citation:
Wyss, C. R., D. Rickenmann, B. Fritschi, J. M. Turowski, V. Weitbrecht, and R. M. Boes (2016), Laboratory flume experiments with the Swiss plate geophone bed load monitoring system: 1. Impulse counts and particle size identification, *Water Resour. Res.*, *52*, 7744–7759, doi:10.1002/2015WR018555.

Received 31 DEC 2015
Accepted 12 AUG 2016
Accepted article online 16 SEP 2016
Published online 9 OCT 2016

Laboratory flume experiments with the Swiss plate geophone bed load monitoring system: 1. Impulse counts and particle size identification

Carlos R. Wyss[1,2], Dieter Rickenmann[1], Bruno Fritschi[1], Jens M. Turowski[3], Volker Weitbrecht[2], and Robert M. Boes[2]

[1]Swiss Federal Research Institute WSL, Birmensdorf, Switzerland, [2]Laboratory of Hydraulics, Hydrology and Glaciology VAW, ETH Zürich, Zürich, Switzerland, [3]Helmholz Centre Potsdam, GFZ German Research Centre for Geosciences, Potsdam, Germany

Abstract We performed systematic flume experiments using natural bed load particles to quantify the effect of different parameters on the signal registered by the Swiss plate geophone, a bed load surrogate monitoring system. It was observed that the number of impulses computed from the raw signal clearly depends on bed particle size, mean flow velocity, bed roughness, and to a minor extent on particle shape. The centroid frequency of the signal resulting from the collision of a bed load particle against the geophone plate was found to be inversely related to particle size but to be less sensitive to variations in mean flow velocity and bed roughness than the signal amplitude, which is also related to particle size. Combining frequency and amplitude information resulted in a more robust identification of the transported particles size over a wide range of sizes than using amplitude information alone.

1. Introduction

Bed load is the fraction of river sediment transport that moves downstream with constant or frequent contact with the bed. Bed load transport is a complex process that has been the subject of numerous scientific studies [*Shields*, 1936; *Einstein*, 1937; *Meyer-Peter and Müller*, 1948]. Monitoring bed load transport is essential for the planning of river engineering projects and comprehension of orogenic erosion and deposition processes [*Burtin et al.*, 2011]. In the past, bed load transport rates were commonly measured directly, by deploying a sediment sampler [*Helley and Smith*, 1971; *Bunte et al.*, 2004], or by surveying sediment retention basins over larger time scales, possibly including larger bed load masses. Portable or fixed slot samplers can also be used to sample transported bed load particles over a part of the stream width [*Hubbell*, 1964; *Reid et al.*, 1980]. Conveyor belt samplers are more sophisticated devices that can continuously collect transported bed load particles over the entire stream width and typically over relatively short time periods [*Emmett*, 1980]. These direct bed load measurement methods are generally time-consuming and technically challenging, especially at high river discharges when coarse bed load particles and most of the bed material is mobilized.

Advances in technology have allowed the development of less intrusive bed load surrogate monitoring techniques, able to record temporal and spatial variations of bed load transport processes [*Gray et al.*, 2010]. These techniques enable continuous measurements of bed load transport fluxes, even at high river discharges where the manual deployment of a device to directly measure bed load transport becomes difficult or impossible. The main element constituting bed load surrogate monitoring techniques is often an acoustic sensor (geophone, accelerometer, hydrophone, microphone, etc.) that continuously measures characteristic properties of bed load transport like the acoustic energy of the noise generated by transported bed load particles [*Belleudy et al.*, 2010] or the number of particle impacts on the stream bed [*Wyss et al.*, 2016a]. Examples of bed load surrogate monitoring devices are magnetic tracers [*Bunte*, 1996], seismometers installed near the river bed [*Burtin et al.*, 2008, 2011; *Roth et al.*, 2015], hydrophones [*Mason et al.*, 2007; *Belleudy et al.*, 2010; *Camenen et al.*, 2012; *Geay*, 2013], the Swiss plate geophone [*Rickenmann et al.*, 2012, 2014], the Japanese pipe hydrophone [*Mizuyama et al.*, 2010a, 2010b], and the acoustic Doppler current

profiler ADCP [*Rennie and Church*, 2010]. For an overview and review of currently used surrogate technologies refer to *Gray et al*. [2010] and *Rickenmann* [2016].

From flume experiments with impact plates, it is known that particle transport mode, i.e., rolling, sliding, or saltating, is a key parameter, the latter being associated with more energy per impact [*Turowski and Rickenmann*, 2009; *Rickenmann et al*., 2012; *Turowski et al*., 2015; *Wyss et al*., 2016a] and generating a higher-frequency signal than the former [*Krein et al*., 2008; *Tsakiris et al*., 2014; *Barrière et al*., 2015]. Also, the energy of the acoustic signal registered by impact-plate bed load monitoring systems increases with increasing bed load transport rate [*Møen et al*., 2010; *Barton et al*., 2010] and there is evidence that this relationship holds until particle concentrations get large enough, such that particle-particle interactions reduce the number of impacts on the sensor plate. This is similar to the cover effect described for bedrock erosion [*Turowski and Rickenmann*, 2009], and to saturation of the acoustic system in which the signals due to multiple particle impacts overlap which makes it difficult or impossible to identify particles individually [*Mizuyama et al*., 2010a]. The frequency of the self-generated noise produced by particle intercollisions decreases with increasing particle size [*Thorne*, 1986; *Belleudy et al*., 2010]. This was also found for the frequency generated by particles colliding onto impact plates [*Etter*, 1996; *Bogen and Møen*, 2003; *Møen et al*., 2010; *Pecorari*, 2013; *Barrière et al*., 2015]. These empirically derived particle-size-frequency relations are supported by a theoretical framework of rigid body radiation [*Thorne*, 2014], and it is interesting that different bed load surrogate monitoring devices produce similar frequency responses [*Rickenmann*, 2016].

Laboratory flume experiments were used to study the signal response of impact-plate bed load surrogate monitoring devices to different transported sediment characteristics and hydraulic conditions. In their flume experiments with natural bed load particles, *Esbensen et al*. [2007] distinguished two major factors, mass flux Q_s and particle size distribution (PSD), to have an effect on the signal recorded by a piezoelectric crystal monitoring the deformation of an impact plate. They were able to develop a model that produced rather accurate estimates of the observed Q_s and PSD. However, their model was based on a multivariate partial least square regression, hindering the identification of the effect that each variable has independently. In the context of industrial applications, *Pecorari* [2013] measured an increase in average power of the acoustic signal with increasing Q_s of solid particles impinging on a flat metal plate. Using a similar setup, *Uher and Benes* [2012] observed that the velocity at which particles collide has no relevant effect on the shape of the frequency spectrum, but it affects the general energy of the signal, which is in agreement with the Hertz theory.

Mizuyama et al. [2010b] performed systematic flume experiments with the Japanese pipe system, a hollow pipe with a microphone measuring air-pressure differences created by transported bed load particles colliding against the steel pipe. They found that for this system also the registered signal varies with mass flux Q_s, bed slope S, particle size D and the location of the particle collision against the pipe. Based on flume experiments with the same system, *Mao et al*. [2016] developed a simple empirical method to extract particle size information, using data registered over 6 channels with different gains for their flume experiments.

From flume experiments with an impact-plate system and a piezoelectric hydrophone as sensor, originally developed by *Krein et al*. [2008], *Barrière et al*. [2015] observed that the D_{50} of the transported bed load was directly proportional to the amplitude A of the first arrival waveform and inversely proportional to the characteristic frequency f_{char} of the signal registered after a single particle impact. This led them to develop a method combining computed A and f_{char} to extract transported D_{50} information. Their results obtained from flume experiments with two different setups converge into the same relation curve, emphasizing that combining amplitude and frequency information can be assembled into a robust method to extract transported particle size information.

The aim of the present study is to investigate important factors affecting the signal response of the Swiss plate geophone. We performed flume experiments to quantify the effects of particle size, bed load material (particle shape), bed roughness, and mean flow velocity on the signal registered by the Swiss plate geophone. The experiments were performed using natural particles from four different streams: Erlenbach (CH), Navisence (CH), Fischbach (AT), and Ruetz (AT). In this first of two companion papers we report on the flume-based relations of the Swiss plate geophone system. We present several methods to compute amplitude and frequency-based characteristic summary values and show how they depend on the investigated parameters.

In a companion paper, the laboratory results obtained here were used to develop flume-based calibration procedures for the Swiss plate geophone.

2. Methods

2.1. Experimental Setup

The experimental work was conducted at the Laboratory of Hydraulics, Hydrology and Glaciology (VAW) at the Swiss Federal Institute of Technology (ETH) Zürich, Switzerland. The effect of particle size D, mean flow velocity V_W, and bed roughness k_s on the signal registered by the Swiss plate geophone system was investigated by performing a series of flume experiments.

Although in principle the functioning of the Swiss plate geophone device is simple, the complex interactions between the device's sensor and the device itself are poorly understood. It is not possible to design and meaningfully use a scaled version of the device in the lab. It follows that to obtain comparable measurements in the lab to those from the field, flume experiments must be carried out with flow and transport conditions as similar as possible to the prototype, i.e., the same device, the same bed load particle sizes, and very similar hydraulic conditions as in the field.

2.1.1. Laboratory Flume

Experiments were performed in a nontiltable flume with a horizontal bed, of dimensions 9000 mm length $\times$ 500 mm width $\times$ 800 mm depth (Figure 1). The adjustable opening of the jet-box [*Schwalt and Hager*, 1992] allowed the setting of the desired flow depth h_w over the Swiss plate geophone. The bottom of the first 5 m of the flume consisted of regular concrete over which most of the particles were transported in sliding mode, as evidenced from qualitative observations during the experiments. The roughness over a length of 2.6 m upstream of the Swiss plate geophone was increased by screwing a wired grid onto the smooth flume-bed. This increased near boundary turbulence and enhanced rolling and saltating transport modes. The diameter of the wire d_w was of 0.5 mm and the spacing of the regular mesh was 2.5 mm. The effective sand roughness of the concrete and the wired grid bed k_s of 5×10^{-5} m and 1×10^{-3} m was estimated by fitting a computed backwater curve to measured values of h_W along the flume as proposed by *Hager* [1999] (Figures S3 and S4 in Supporting Information). A vertical silicon joint of 1 cm width was the only element connecting the steel carrying structure of the flume with the Swiss plate geophone to acoustically isolate the geophone system from the expected flume vibrations induced by the moving particles.

2.1.2. Swiss Plate Geophone

The Swiss plate geophone consists of a geophone sensor (GS-20DX by Geospace technologies) mounted underneath a stainless steel plate of dimensions 496 mm width $\times$ 360 mm length $\times$ 15 mm thickness installed on the river bed [*Rickenmann and Fritschi*, 2010; *Rickenmann et al.*, 2012; *Wyss et al.*, 2016a]. The geophone sensor produces a voltage proportional to the velocity at which the plate vibrates following the kinetic impact of a bed load particle moving over the plate [*Turowski et al.*, 2013].

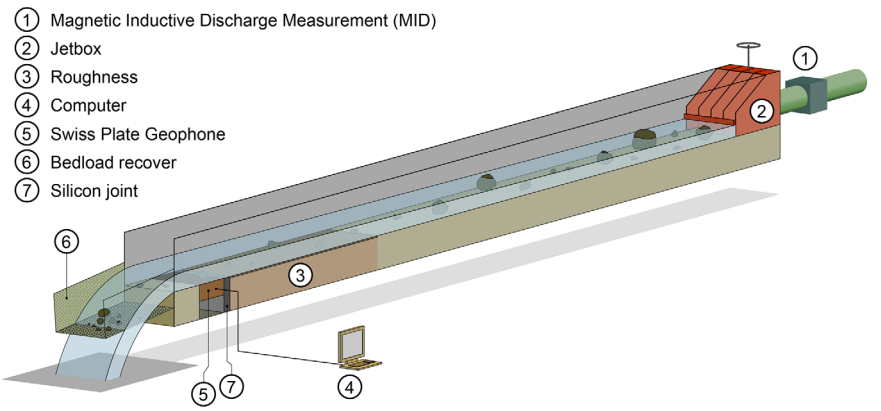

Figure 1. Schematic of the glass-walled flume. (1) Discharge in the flume was measured with Magnetic Inductive Discharge Measurements (MID). (2) The depth of the flow was regulated with a jet-box. (3) The roughness over the lowermost 2.6 m of the flume's bed was increased by installing a wired grid. The computer (4) continuously stored the raw signal produced by the Swiss plate geophone (5) located 7.5 m downstream of the jet-box. (6) A mesh was installed at the end of the flume to recover the bed load particles. (7) A silicon joint of 1 cm width acoustically isolates the Swiss plate geophone from flume vibrations.

Table 1. Coefficient a_{stream}, Exponent b_{stream} and Respective Coefficient of Determination R^2 of Equation (1) for the Four Streams, Where the Units of D Are in mm and G_m in g

Stream	a_{stream}	b_{stream}	R^2
Erlenbach	9.44	0.34	0.93
Navisence	9.61	0.33	0.93
Fischbach	8.83	0.34	0.93
Ruetz	9.43	0.33	0.91

The signal registered by bed load surrogate monitoring devices is complex and contains a broad spectrum of information [*Krein et al*., 2008]. In the case of the Swiss plate geophone, the vertical deformation velocity of the center of the steel plate is continuously sampled at a rate of $f_s = 10$ kHz by the geophone sensor system. The manner the plate vibrates, i.e. how fast and with how much energy, depends on its proper characteristics and on collision characteristics like force, collision location, and impact style and angle of the moving bed load particle against the steel plate [*Turowski et al*., 2013; *Barrière et al*., 2015].

2.2. Experimental Program

Flume experiments were performed with bed load material from four different gravel-bed streams in mountain areas mentioned in section 1.

2.2.1. Size and Weight of Bed Load Particles

To study the effect of particle size D on the signal registered by the Swiss plate geophone, particle weight G_m was used to define nine particle-size classes and particles from all these classes were used in the flume experiments. The length of the three axis of at least 460 bed load particles and their corresponding mass was measured for bed load material collected from the four streams. This allowed attributing particle shape according to 10 descriptive classes [*Sneed and Follk*, 1958; *Benn and Ballantyne*, 1993] (Figure S2) and establishing a relationship between D (measured b axis of the particle) and G_m which is well fitted by a power law function [*Ibbeken*, 1974; *Bunte and Abt*, 2001]

$$D_{stream} = a_{stream} \cdot G_m^{b_{stream}}, \quad (1)$$

where the subscript "stream" stands for Erlenbach, Navisence, Fischbach, or Ruetz (Table 1).

The site-dependent coefficient a_{stream} and exponent b_{stream} in equation (1) (Table 1) were used to compute mean particle size D_m corresponding to G_m for the four streams (Table 2). Bed load particles were sorted manually by weight and included in particle-size class j if their weight was in the range of $G_{m,j} \pm 30\%$ and thus the particle size within a class j varied by $(D_m \pm 30\%)^{b_{stream}}$ which is on average about $\pm 10\%$. Therefore, the size of the largest particle within a given size class D_{max} is on average 10% larger than the mean particle size of that same size class, i.e., $D_{max} \approx 1.1 \cdot D_m$.

2.2.2. Flume-Based Relations

Our flume experiments were designed to quantify the effect of mean water flow velocity V_W [*Rickenmann et al*., 2014], particle size D [*Etter*, 1996; *Turowski and Rickenmann*, 2009; *Rickenmann et al*., 2014; *Turowski et al*., 2015; *Wyss et al*., 2016a], and bed roughness k_s on the signal registered by the Swiss plate geophone.

For this study, a flume-based relation is defined as the mathematical function between a computed characteristic signal value (see section 2.3) and bed load particle size. This facilitates the comparison of the relations obtained for different mean flow velocities V_W and with natural bed load particles from different gravel-bed streams. A flume-based relation was established by performing 5–50 experimental runs R for each particle size and stream material (Table 3). In each run, 5–20 bed load particles from a given stream were fed simultaneously by hand 0.5 m downstream of the jet-box into the flow or 7 m upstream of the geophone plate, for a given V_W. The number of individual runs R, as well as the number of particles NG per R varied based on particle size (Table 3). A decreasing number of particles per run NG/R was selected such that a maximum total weight of about $M_{b,flume} = 10$ kg per run was not

Table 2. Mean Particle Size D_m Computed With Equation (1) for the Four Streams

Particle-Size		Erlenbach	Navisence	Fischbach	Ruetz
Class j	G_m [g]	$D_{m,Eb}$ [mm]	$D_{m,Na}$ [mm]	$D_{m,Fi}$ [mm]	$D_{m,Ru}$ [mm]
1	8	19.1	19.1	17.9	18.7
2	16	24.2	24.0	22.7	23.5
3	32	30.7	30.2	28.7	29.6
4	64	38.8	37.9	36.3	37.2
5	128	49.1	47.7	46.0	46.8
6	256	62.2	59.9	58.2	58.8
7	512	78.7	75.3	73.6	73.9
8	1024	99.7	94.7	93.2	92.9
9	2048	126	119	118	117

Table 3. Number of Experimental Runs R for Each Particle-Size Class j Used to Establish One Calibration Relation[a]

Particle-Size Class j	$\bar{G}_{m,j}$[b] [g]	NG_{total}[c]	NG/R	R	$M_{b,flume}$ [kg]	G_{total} [kg]
1	8	1000	20	50	0.16	8
2	16	1000	20	50	0.32	16
3	32	1000	20	50	0.64	32
4	64	400	20	20	1.28	25.6
5	128	400	20	20	2.56	51.2
6	256	400	20	20	5.12	102
7	512	100	10	10	5.12	51.2
8	1024	50	10	5	10.24	51.2
9	2048	25	5	5	10.24	51.2
Total		4375		230		388.4

[a]Particle weight G_m was used to sort the bed load particles gathered in the field into nine size classes. The number of particles NG per R with a mass of $M_{b,flume}$ and the total number of transported particles NG_{total} over the Swiss plate geophone depended on particle-size class j.

[b]To sort the bed load into the different particle-size classes, particles weighing in the range of $G_{m,j} \pm 30\%$ were attributed to particle-size class j.

[c]Total number of transported particles over the Swiss plate geophone used for establishing of a calibration relation.

exceeded when feeding the bed load material into the flume.

2.2.3. Flow Conditions in the Flume

The same experimental series were repeated at different mean flow velocities V_W with material from the four gravel-bed streams (Table 4). Flume experiments were conducted under supercritical flow, in view of a substantial fraction of considered particle sizes not being transported over the flat horizontal flume bed under subcritical flow conditions. It is known from laboratory and field observations that mean flow velocity V_W has an important effect on the resulting calibration of the Swiss plate geophone [*Hegglin*, 2011; *Rickenmann et al*., 2014]. We therefore replicated typical field V_W values in the flume to perform these experiments. Due to technical limitations in the laboratory, with the exception of the Erlenbach, the water depth h_w in the flume was typically smaller than in the field [*Wyss et al*., 2016b]. The vertical velocity profiles are unknown both in the field and in the flume. A detailed discussion of the comparison between field and flume conditions is given in the companion paper [*Wyss et al*., 2016b].

2.3. Signal Characteristics

Signal characteristic or summary values contain simplified and discrete information that helps to interpret the complex raw signal which contains a broad spectrum of information in the amplitude and frequency domain.

2.3.1. Impulses

The Swiss plate geophone is a robust bed load surrogate monitoring system that has been successfully used to quantify bed load transport with signal impulse counts in several mountain streams [*Rickenmann et al*., 2014]. The number of impulses I are defined as the number of times the raw signal exceeds a predefined threshold of 0.1 V. This threshold is estimated to be at least 1 order of magnitude larger than the signal generated by highly turbulent flows without bed load transport in the field [*Wyss et al*., 2016a] and is therefore unlikely to interfere with background noise. For the Swiss plate geophone measurements, *Rickenmann et al*. [2012, 2014] proposed a linear relation between I and total transported bed load mass M_{tot}

$$I = k_b \cdot M_{tot}\,, \tag{2}$$

where k_b is a field-site dependent constant.

To investigate the effect of particle size on I, we can define a relation for each particle-size class j (Table 3) [*Rickenmann et al*., 2014] as

$$k_{b,j} = \frac{I_{flume,j}}{M_{bj,flume}}\,, \tag{3}$$

where $I_{flume,j}$ are the number of impulses registered by the flume's geophone during the passage of all bed load particles of size j over the steel plate with their total mass $M_{bj,flume}$.

Table 4. Main Flow Conditions of Flume Experiments Over the Swiss Plate Geophone

Bed Load Material	V_W [m/s]	h_w[a] [m]	Fr[b]	Re[c]
Erlenbach	1.5	0.10	1.79	1.07e5
	2.5	0.10	2.99	1.79e5
	3.5	0.10	4.18	2.50e5
	4.7	0.07	6.42	2.57e5
Navisence	1.6	0.10	1.91	1.14e5
	2.0	0.17	2.01	2.02e5
	3.0	0.10	3.58	2.14e5
Fischbach	1.0	0.10	1.19	7.14e4
	2.0	0.10	2.39	1.43e5
	3.0	0.10	3.58	2.14e5
Ruetz	1.0	0.10	1.19	7.14e4
	2.0	0.10	2.39	1.43e5
	3.0	0.10	3.58	2.14e5

[a]Water depth h_w was measured with a water gauge fixed to the flume's wall at the level of the Swiss plate geophone.

[b]The Froude number Fr was computed as $V_W/\sqrt{g \cdot R_h}$, where R_h is the hydraulic radius and $g = 9.81$ m/s is the gravitational acceleration.

[c]The Reynolds number Re was computed as $V_W \cdot R_h/\nu$, where $\nu = 1\,e^{6}$ [m^2/s] is the kinematic viscosity of water at a temperature of 20°C.

2.3.2. Packets

We assume that the complete response of the geophone signal following a single

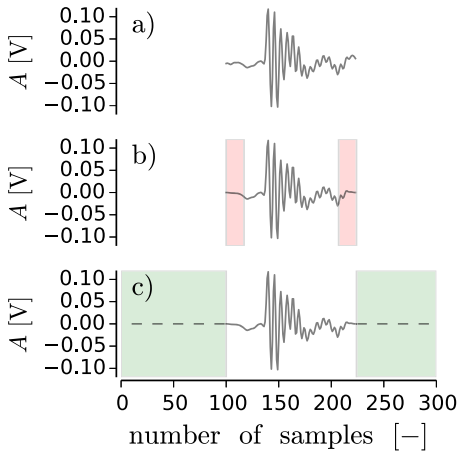

Figure 2. Illustration of the preprocessing for one packet before computing $f_{centroid}$. (a) Original extracted packet from the signal. (b) Cosine taper applied over 30% of the packet (read area, 15% each edge). (c) Zero padding beyond the edges of the packet until the number of samples equals f_s (green area).

particle impact over the Swiss plate geophone is contained within a "packet" [*Wyss et al.*, 2016a]. The identification of packets is based on the computation of the envelope function with a Hilbert transform. Like the number of impulses, the number of registered packets P have been used to quantify bed load transport rates [*Wyss et al.*, 2016a].

2.3.2.1. Maximum Amplitude

The maximum amplitude $A_{max,P}$ is defined as the maximum positive registered voltage within a packet. In contrast to the number of registered impulses I and packets P, $A_{max,P}$ has been found to contain information about the size of the transported bed load particle [*Rickenmann et al.*, 2014; *Wyss et al.*, 2016a].

2.3.2.2. Spectral Centroid Frequency

The frequency at which the geophone plate vibrates depends on the size of the colliding particle [*Etter*, 1996; *Bogen and Møen*, 2003; *Barrière et al.*, 2015; *Rickenmann*, 2016]. The spectral centroid $f_{centroid}$ was chosen to characterize the frequency spectrum of a packet. It indicates the center of mass of the spectrum and is computed as

$$f_{centroid} = \frac{\sum f_n \cdot A_{FFT,n}}{\sum A_{FFT,n}}, \tag{4}$$

where f_n [Hz] is the spectrum frequency and $A_{FFT,n}$ [V·s] is its corresponding Fourier amplitude computed with the Fast Fourier Transform (FFT). The FFT algorithm operates only over signals containing at least as many samples or data points as its f_s. Consequently, before applying the FFT, the packet is preprocessed in two steps: cosine taper and zero-padding (Figure 2). To compute a more accurate frequency spectrum, a cosine taper is applied at the edges of the packet to smooth the transition to the straight line (dashed line in Figure 2c) concatenated by zero padding. A FFT is then applied over the processed packet to compute A_{FFT} which in turn is used to compute $f_{centroid}$ (equation (4)).

3. Results

3.1. Impulses

From our experiments it was found that the impulse-diameter coefficient k_{bj} varies with particle size, flow velocity, and stream-bed material. For increasing particle sizes larger than about 20 mm k_{bj} increases to reach a maximum and then decreases again (Figure 3). Considering all four streams, the maximum value of the flume impulse-diameter relations $k_{bj,max}$ decreases by a factor of about 5 when increasing the mean flow velocity V_W from 1 to about 5 m/s (Figures 3 and 4a). Furthermore, the corresponding particle size of $k_{bj,max}$, $D_m(k_{bj,max})$ decreases with increasing V_W (Figures 3 and 4b), implying that smaller particles tend to trigger relatively more impulses per transported mass at higher V_W.

The fitted curve for all the flume-based impulse-diameter relations shown in Figure 3 represents a scaled probability density distribution of the generalized Frechet distribution as described by *Abd-Elfattah and Omima* [2009]. The choice of the Frechet distribution is essentially arbitrary, but it fits the flume measurements very well, with a maximum relative standard error σ_e of 16% (reported in Table 5). The Frechet curves also help to visually better distinguish the results obtained for different V_W (Figure 3).

The impulse-diameter relation curves $k_{bj} = f(D)$ (Figure 3) were fitted with the generalized Frechet distribution [*Abd-Elfattah and Omima*, 2009]

$$f(x,\Omega,\alpha,\lambda,\sigma) = \Omega \cdot \alpha \cdot \lambda \cdot \sigma^{\lambda} \left[1 - \exp\left\{-\left(\frac{\sigma}{x}\right)^{\lambda}\right\}\right]^{\alpha-1} \cdot x^{-(\lambda+1)} \cdot \exp\left\{-\left(\frac{\sigma}{x}\right)^{\lambda}\right\}, \tag{5}$$

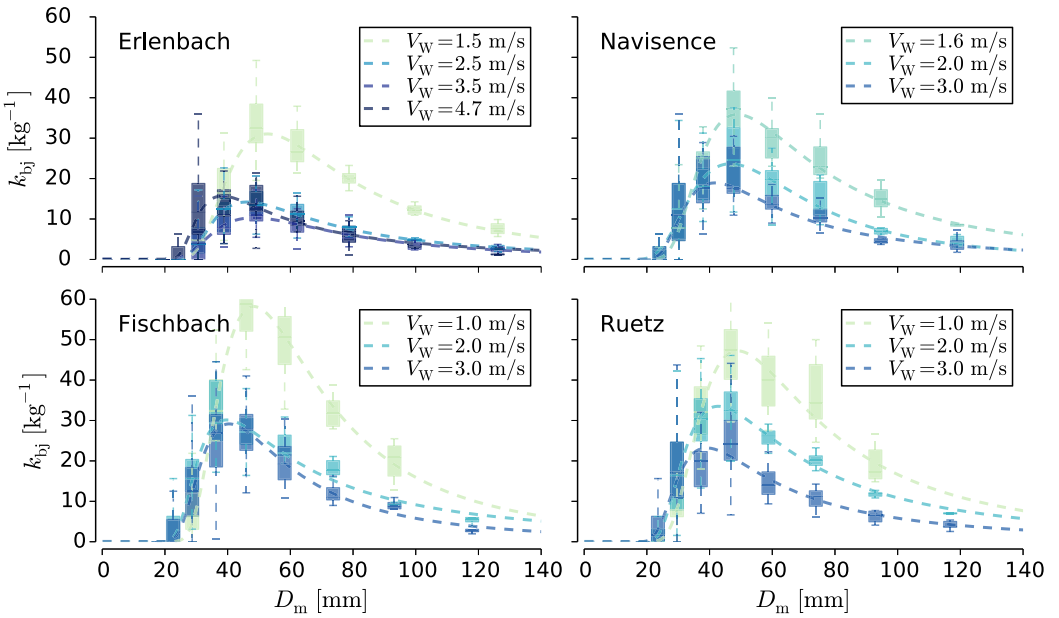

Figure 3. Impulse-diameter relation curve, representing recorded impulses per unit bed load mass k_{bj} as a function of mean particle-size D_m, for different mean flow velocities V_W.

where $\Omega > 0$ is a scaling parameter, $\sigma > 0$ is a scale or spreading parameter, and $\alpha > 0$ and $\lambda > 0$ are shape parameters. The nonlinear least squares fitted parameters in equation (5) for the impulse-diameter relations are given in Table 5. With the purpose of developing a field-independent calibration of the Swiss plate geophone, the four parameters fitted in equation (5) can be estimated merely from the mean flow velocity (Figure 5).

These impulse-diameter relations are reported here in some detail because they were applied in a companion paper to geophone calibration measurements from the four field sites, from which bed load particles were used for the flume experiments of this study. In particular, flume-based calibration procedures were developed for the Swiss plate geophone and compared with the field calibration measurements [*Wyss et al.*, 2016b].

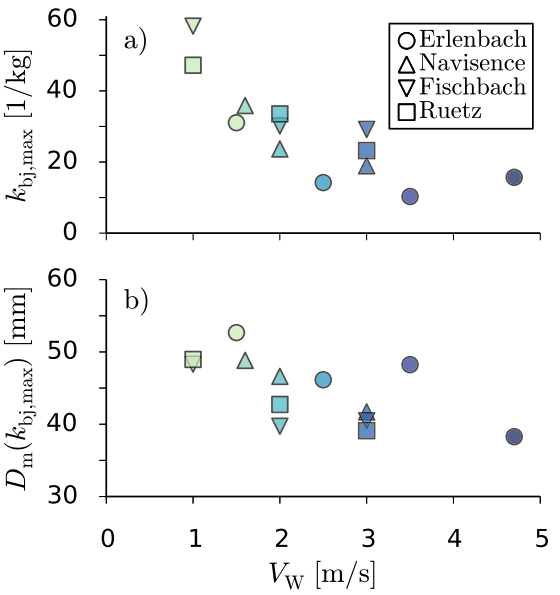

Figure 4. (a) Maximum value of the fitted calibration curve in Figure 3, $k_{bj.max}$, for all streams and as a function of mean flow velocity V_W. (b) Particle-size $D_m(k_{bj.max})$ corresponding to $k_{bj.max}$, as a function of V_W.

3.2. Amplitude and Frequency

The maximum amplitude of a packet $A_{max,P}$ increases significantly with increasing particle size and slightly with increasing mean flow velocity V_W (Figure 6). Power law functions were fitted to the median values of $A_{max,P}$ to better visualize differences of the dependent variables with particle size D and mean flow velocity V_W, and they are reported quantitatively in Supporting Information (Table S1). The general equation best representing all flume cases is $D_m = 67.5 \cdot A_{max,P}^{0.40}$ with an $R^2 = 0.95$. In contrast to $A_{max,P}$, the representative frequency $f_{centroid}$ of a packet decreases with increasing particle size (Figure 7 and Table S2), but shows only a weak dependency on V_W.

Similar as in the study of *Barrière et al.* [2015], we defined a power law relation for the flume data with particles from the four study streams, by combining amplitude and frequency information to particle size as

Table 5. Fitted Parameters in Equation (5)

Bed Load Material	V_w [m/s]	Ω [1/kg]	α	λ	σ	σ_e[a]
Erlenbach	1.5	2283	0.55	2.95	54.3	0.089
	2.5	1111	0.31	3.54	44.0	0.047
	3.5	808	0.55	2.60	50.8	0.103
	4.7	1202	0.16	4.82	34.4	0.120
Navisence	1.6	2705	0.47	2.96	49.4	0.052
	2.0	1397	1.44	1.92	61.3	0.125
	3.0	1243	0.40	3.22	41.1	0.103
Fischbach	1.0	3446	0.61	3.12	50.0	0.049
	2.0	2644	0.19	3.91	36.2	0.081
	3.0	1592	0.47	3.37	40.3	0.073
Ruetz	1.0	3455	0.52	2.88	50.2	0.081
	2.0	2755	0.30	3.23	41.0	0.057
	3.0	1587	0.33	3.31	37.7	0.163

[a]Relative standard error σ_e defined as the standard deviation of the difference between the estimated and the measured values, divided by the mean of the measured values (k_{bj}).

$$D_m = K \frac{A^a}{f_{centroid}^b}, \tag{6}$$

where K is a constant. From their flume experiments, *Barrière et al*. [2015] found optimum values for the exponents a and b in equation (6) of 0.39 and 0.86, respectively. For the data of our flume experiments, the coefficient of determination R^2 was computed for a function in the form of equation (6) by varying a and b to find an optimum value. Optimum a and b parameters in equation (6) appear to vary somewhat with bed load material properties and less with flow velocity (Figure 8).

The exponents proposed by *Barrière et al*. [2015], i.e., $a = 0.39$ and $b = 0.86$, would result in high R^2 values (equation (6)) for our flume experiments. However, our global optimum, considering all flow velocities and bed load materials (Table 4), is found at $a_{glob} = 0.23$ and $b_{glob} = 0.53$ (Figure 8) with a general $R^2 = 0.97$ and global constant $K_{glob} = 2670$ (Figure 9), computed by averaging the case specific optimum K values for each flow condition (Table 4) reported in Supporting Information (Tables S3–S6).

3.3. Packet Duration

The duration $\Delta_{t,P}$ of the registered packet following the impact of a bed load particle on the Swiss plate geophone is a summary value of the signal that correlates well with bed load transport rates for the Erlenbach, over a very wide range of transport intensities, i.e., for q_s in the range of 10^{-4} to 1 kg/m s [*Wyss et al*., 2016a]. Our flume data show that the packet duration $\Delta_{t,P}$ increases with particle size and that it is influenced somewhat by mean flow velocity V_W (Figures 10 and Table S8 of Supporting Information).

Table 6. Discrepancy Ratio Between Estimated and Measured Particle Size $r_{A_{max}/f_{centroid},D_m}$[a]

		$r_{A_{max}/f_{centroid},D_m}$								
Bed Load Material	V_w [m/s]	$D_{m,1}$ [1/kg]	$D_{m,2}$	$D_{m,3}$	$D_{m,4}$	$D_{m,5}$	$D_{m,6}$	$D_{m,7}$	$D_{m,8}$	$D_{m,9}$
Erlenbach	1.5	1.10	1.05	0.96	0.90	0.90	0.84	0.84	0.86	0.81
	2.5	1.10	1.04	0.98	0.93	0.90	0.87	0.85	0.80	0.79
	3.5	1.08	0.99	0.96	0.97	0.91	0.81	0.89	0.93	0.74
	4.7	1.19	1.08	1.06	1.01	0.97	0.97	1.00	0.88	0.83
Navisence	1.6	1.11	1.09	1.02	0.95	0.94	0.94	0.97	1.01	1.06
	2.0	1.14	1.06	1.04	0.99	0.97	0.97	1.09	1.08	1.10
	3.0	1.14	1.08	1.10	1.03	0.96	1.01	1.17	1.16	1.12
Fischbach	1.0	1.14	1.09	1.05	0.98	0.94	0.90	0.88	0.91	-
	2.0	1.22	1.17	1.15	1.07	1.03	1.08	1.06	1.21	1.09
	3.0	1.22	1.16	1.09	1.13	1.11	1.12	1.24	1.22	1.12
Ruetz	1.0	1.12	1.08	1.01	0.97	0.93	0.91	0.88	0.95	-
	2.0	1.16	1.14	1.08	1.03	1.07	1.04	1.19	1.08	1.01
	3.0	1.23	1.15	1.12	1.02	1.09	1.14	1.17	1.22	1.04

[a]The estimates where computed with global optima (K_{glob}, a_{glob}, and b_{glob} in equation (6)).

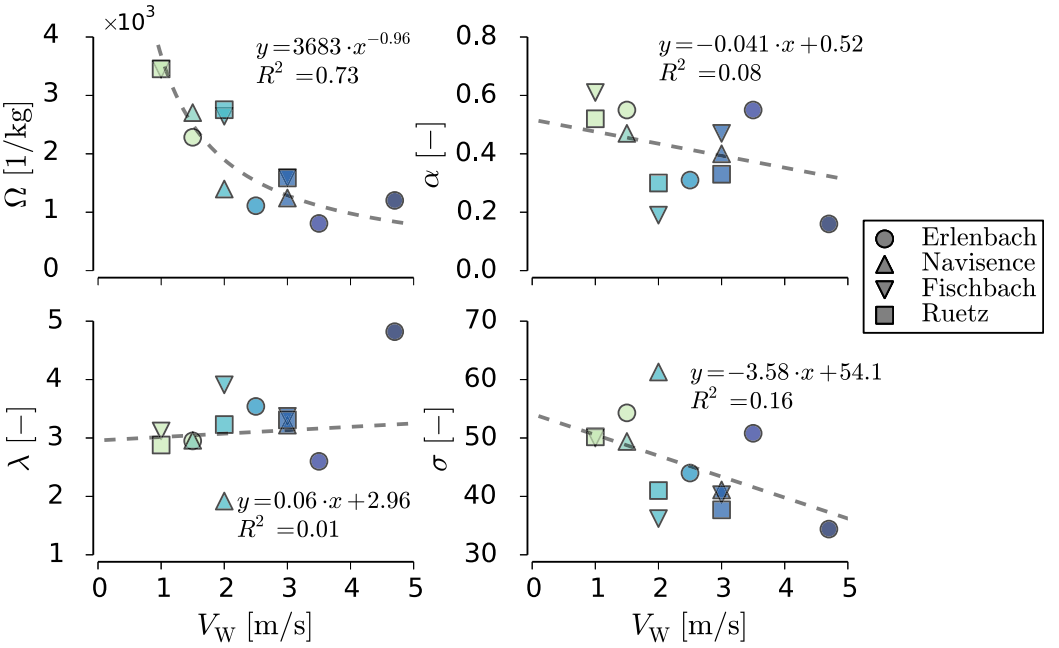

Figure 5. The impulse versus grain-size relations were fitted with a generalized Frechet distribution. This figure shows a fitted trend line for each of the four parameters that define the generalized Frechet distribution (equation (5)) as a function of mean flow velocity V_W only.

4. Discussion

4.1. Particle Size and Mean Flow Velocity

The smallest particles that collide strongly enough to register an impulse, marking the detection limit of the Swiss plate geophone system, are around D_m=20 mm. This detection threshold is an estimation based on (1) the smallest particles ranging on average from 17.9 to 19.1 mm depending of bed load material (Table 2) generating 0 impulses and (2) the next larger particle-size class (ranging from 22.7 to 24.2 mm) generating between 0 and 15 impulses (Figure 3). This detection threshold is in agreement with the analysis of the raw geophone signal at the Erlenbach field site where the probability to detect a

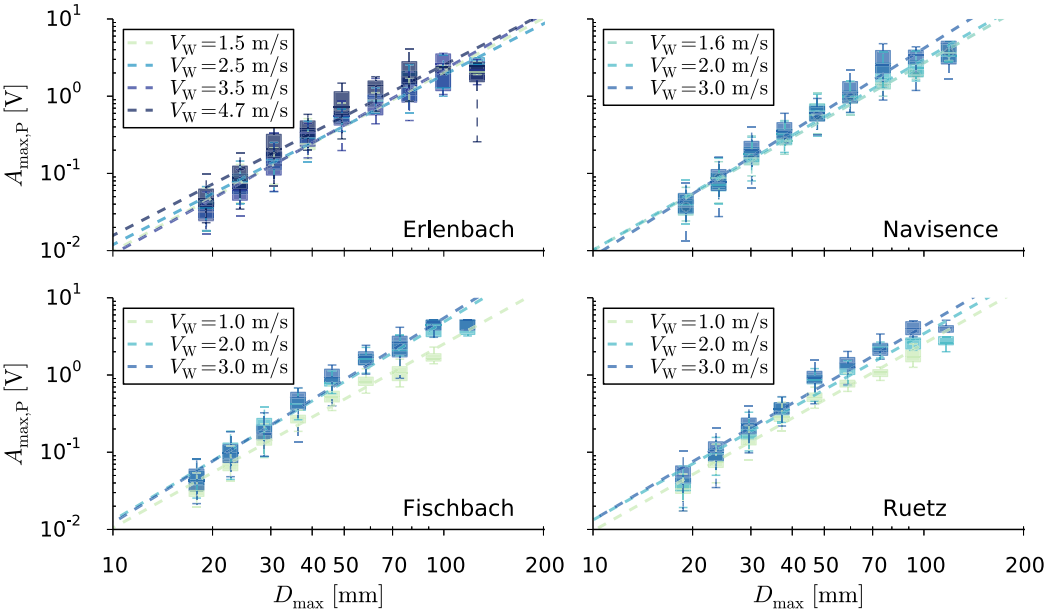

Figure 6. Maximum amplitude of a packet $A_{max,P}$ as a function of mean particle-size D_m, for different mean flow velocities V_W.

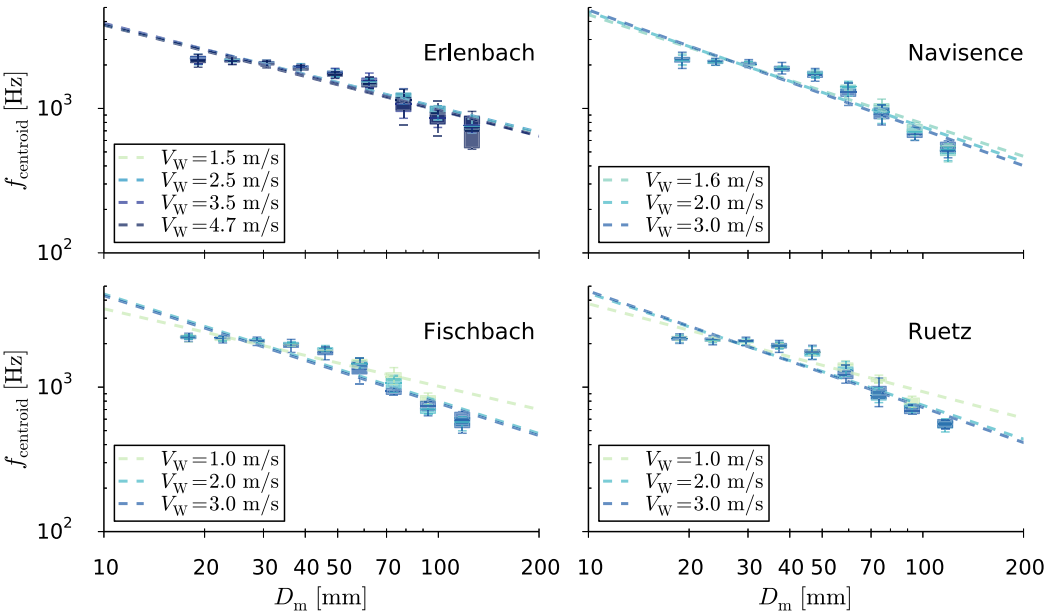

Figure 7. Representative frequency $f_{centroid}$ as a function of mean particle-size D_m, for different mean flow velocities V_W.

particle of mean size in the range from 12.3 to 17.4 to 21.8 mm changes from 1 to 5 and to 8%, respectively [*Wyss et al.*, 2016a, Figure 8]. Above this detection threshold, the shape of the impulse-diameter relation (Frechet curve) is comparable for different flow velocities V_W (Figure 3) and is the result of two effects: An increase in the amplitude $A_{max,P}$ (and thus a higher detection probability) is observed for the increasing part of the coefficient k_{bj} with increasing particle size D. The decrease of k_{bj} after the maximum, which is in the range of 40 mm $< D_m <$ 60 mm, can be explained by the decreasing number of transported particles per unit mass with increasing particle size.

There is a clear decrease in the error bars of k_{bj} with increasing D, the variability being of about $\pm$100% for smaller particles and $\pm$50% or smaller for larger particles (Figure 3). We believe that this result is due to two main reasons. The first reason is related to decreasing signal amplitude with increasing distance between the impact location and the geophone sensor [*Turowski et al.*, 2013], which is located underneath the center of the plate. Indeed, the largest transported particles cover about 35% of the plate's and the flume's width while the smaller ones cover only about 5% of the width and are therefore more likely to collide toward the edges of the plate. The second reason is related to changing transport mechanism with increasing particle size. Flume experiments have shown that bed load particles are more likely to be transported in saltation mode than in rolling mode, as the Shields parameter θ increases [*Hu and Hui*, 1996; *Ancey et al.*, 2002; *Auel et al.*, 2015]. The lack of velocity profile measurements and the particular flow conditions in the horizontal flume characterized by the presence of a backwater curve (nonuniform flow depth h_W illustrated in Figures S4 and S5 of in Supporting Information) makes it difficult to estimate effective θ values for the different particle-size classes (Table 2) over the Swiss plate geophone. Still, the large error bars of k_{bj} for smaller D could be associated to particles being transported in both rolling and saltating mode, while from qualitative observations the larger particles in the flume were almost exclusively transported in sliding mode and, thus, generated a less variable signal.

With the exception of the impulse-diameter relation obtained with bed load material from the Erlenbach at V_W=4.7 m/s, the maximum in the fitted Frechet curves of the impulse-diameter relations decreases and is shifted to smaller D_m with increasing V_W. The most obvious effect of increasing flow velocity is a general decrease in number of impulses. We propose that this is due to fast moving particles being less likely to collide against the Swiss plate geophone than slower moving ones, which are more frequently in contact with the bed. A secondary effect concerns the slight shift of $D_m(k_{bj,max})$ toward a smaller particle size (Figure 4b). We hypothesize that smaller particles that are transported faster collide with more energy against the Swiss plate geophone than slower particles, probably due to increasing saltation height [*Auel et al.*, 2015] or

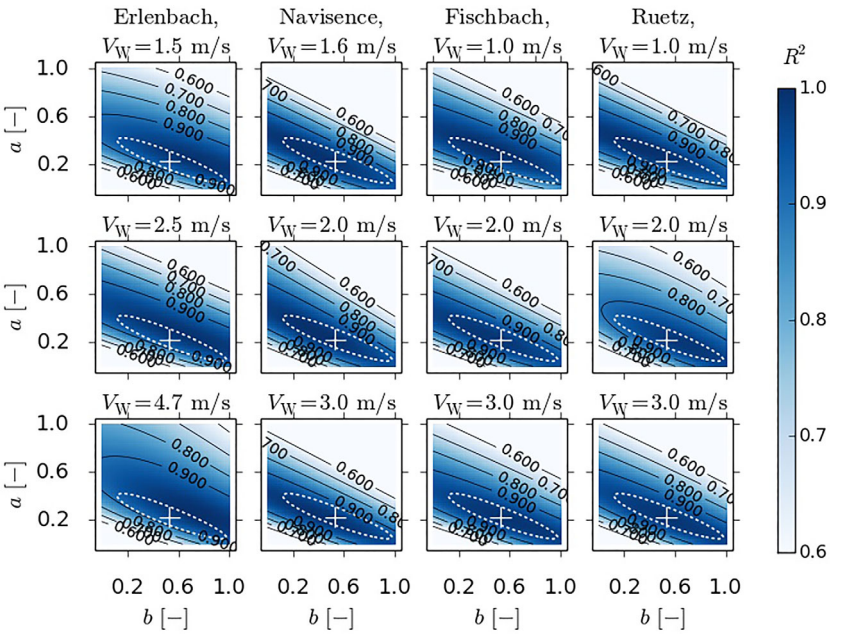

Figure 8. Coefficient of determination R^2 as a function of exponents a and b in equation (6). The white cross indicates the global optimum coefficients a_{glob} and b_{glob} obtained by summing the normalized case-specific R^2 values. The white dashed line delineates the region for which values of the normalized global optimum are greater than 98%.

increasing turbulence with increasing V_W. This effect is noticeable in Figure 6 as the maximum registered amplitude A_{max} of a packet slightly increases with increasing V_W.

An increase in the amplitude of the signal registered by the Swiss plate geophone with increasing particle size (Figure 6) was previously observed in the field [*Rickenmann et al*., 2014]. A method based on this relation was developed to determine bed load transport rates by particle-size fractions at the Erlenbach stream [*Wyss et al*., 2016a]. A relation between signal amplitude and particle size was also reported for other impact plate bed load surrogate monitoring systems [*Etter*, 1996; *Beylich and Laute*, 2014; *Barrière et al*., 2015]. Similarly, for flume experiments with a Japanese pipe-hydrophone, the amplitude of the registered signal increases linearly with the momentum of the colliding particles [*Taniguchi et al*., 1992; *Goto et al*., 2014].

4.2. Effect of Bed Roughness and Particle Shape

Bed morphology and bed roughness play an important role in determining particle transport mode, i.e., sliding, rolling, or saltating [*Lajeunesse et al*., 2010]. In turn, the signal registered by the Swiss plate geophone is also affected by the mode of transport of bed load particles [*Turowski and Rickenmann*, 2009]. To quantify this effect for two very different conditions, supplementary experiments were performed with a smooth and flat PVC plate as bed-roughness element in the flume over the length of 2.6 m upstream of the geophone plate (Figure 1), with bed load material from the Erlenbach stream. The characteristic parameters determined with either the smooth bed S or the rough bed R (with the wire mesh) are compared with each other in Figure 11.

The effect of bed roughness is substantial. It is evident that the number of impulses per transported mass k_{bj} and the maximum amplitude $A_{max,p}$ are generally smaller for a smooth than for a rough bed (Figures 11a and 11b, respectively). The centroid frequency $f_{centroid}$ is less affected by bed roughness than k_{bj} and A_{max}. Divergence in $f_{centroid}$ is evident mainly for particles larger than 80 mm (Figure 11d). Combining amplitude and frequency information with the optimum parameter combination obtained for the rough-bed case (equation (6) and Figure 8) results in an important overestimation of the transported D_m (Figure 11c).

4.3. Particle Size Identification

The characteristic frequency of the signal corresponding to a single particle impact $f_{centroid}$ is less sensitive to varying V_W values than the impulse-diameter parameter k_{bj} or the maximum registered packet amplitude

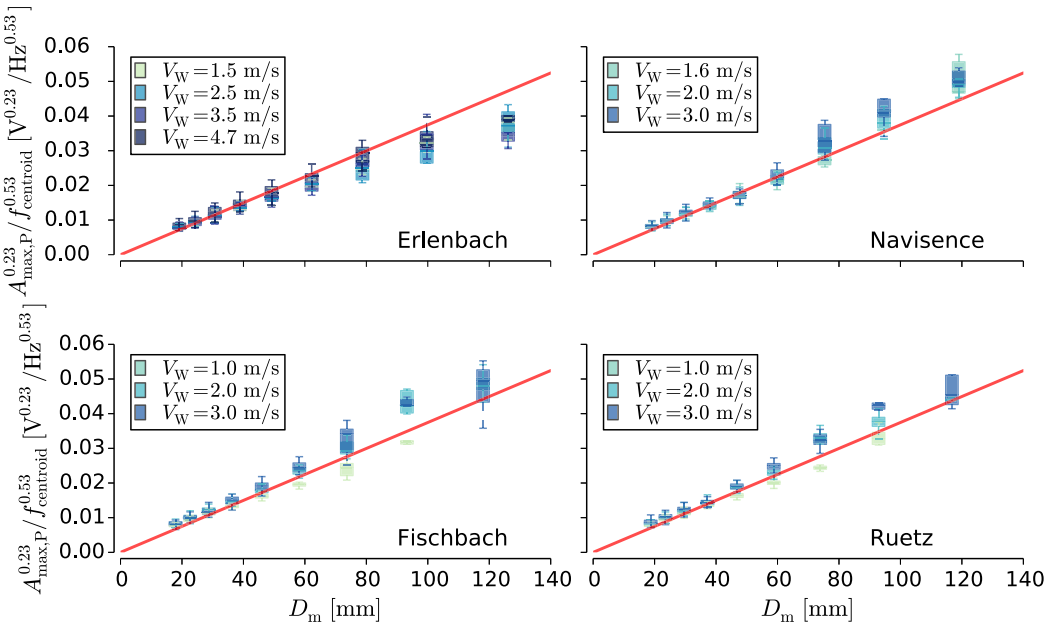

Figure 9. $A_{max,P}^{a_{glob}}$ divided by $f_{centroid}^{b_{glob}}$ as a function of particle-size D_m. The continuous red line indicates a stream-independent relationship obtained with K_{glob} = 2670 in equation (6). The discrepancy ratio between estimated (red dashed line) and median measured particle sizes $r_{A_{max}/f_{centroid},D_m}$ indicates the accuracy of particle size predictions for a global, stream and flow velocity independent approach (Table 6). The case-specific optimum exponents and constant K in equation (6) are reported in Supporting Information.

$A_{max,P}$ (Figures (3 and 6), and 7, respectively). This result is in agreement with observations from laboratory experiments for which no significant effect was observed on the shape of a frequency spectrum by varying the velocity of solid particles impinging on a flat plate [*Uher and Benes*, 2012]. The decrease in centroid frequency $f_{centroid}$ (Figure 7) with increasing particle size is also observed for different bed load surrogate monitoring techniques [*Belleudy et al*., 2010; *Uher and Benes*, 2012; *Barrière et al*., 2015] and is supported by a theoretical framework of rigid body radiation based on the Hertzian impact theory developed by *Thorne* [1986, 2014] and *Rickenmann* [2016].

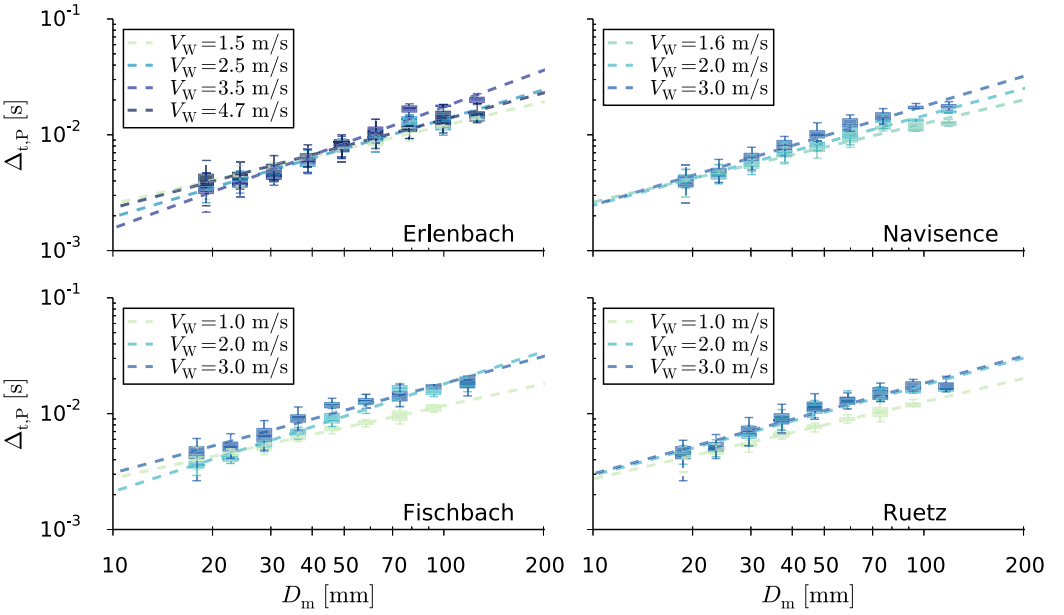

Figure 10. The duration of a packet t_p as a function of mean particle size D_m.

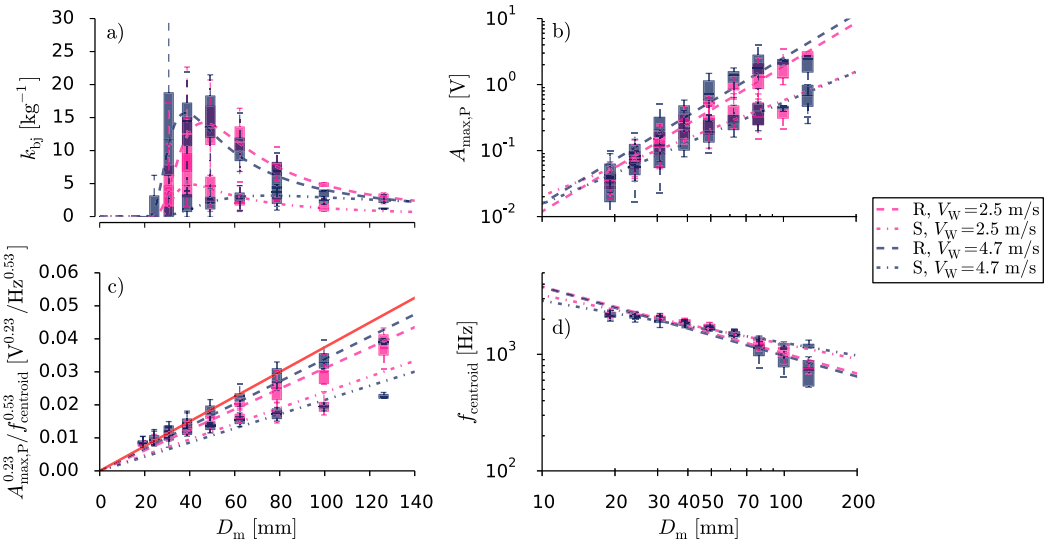

Figure 11. Resulting characteristic values as a function of mean particle size D_m from experiments performed with a rough bed R and a smooth bed S and with bed load material from the Erlenbach stream at two different mean flow velocities V_W. (a) The number of impulses per transported mass k_{bj}. (b) Maximum amplitude of the registered packets $A_{max,P}$. (c) Maximum packet amplitude divided by its centroid frequency ($A_{max,P}^{a_{glob}}$ divided by $f_{centroid}^{b_{glob}}$). The continuous red line indicates a stream-independent relationship obtained with K_{glob}=2670 in equation (6). (d) Centroid frequency within a packet $f_{centroid}$.

There is some systematic deviation between the data and the fitted power law function linking particle size to $A_{max,P}$ and $f_{centroid}$ (Figures 6 and 7, respectively). For $A_{max,P}$, the deviation is essentially only present for the largest transported particle-size class, i.e., $D > 100$ mm (Table 2). It is suspected that the largest particle-size class, which is generally larger than the flow depth h_w in all experiments (Table 4), induces relatively lower $A_{max,P}$ mainly because in contrast to the smaller particle-size classes, it is known from qualitative observations that essentially all particles were transported in sliding mode. For $f_{centroid}$ a clear deviation appears in the range of the smallest particle-size classes (D_m smaller than about 40 mm). A likely explanation for this is that the highest frequencies that can be reasonably sampled with the deployed geophone sensor are in the range of 2.5 kHz. This was qualitatively confirmed by preliminary flume experiments using an accelerometer instead of a geophone sensor mounted on the same impact plate, the accelerometer being able to better pick up higher frequencies for particle sizes smaller than 40 mm.

For the Swiss plate geophone system, a particle size identification using both amplitude and frequency information appears to be more independent of V_W and particle shape (equation (6) with $a = 0.23$ and $b = 0.53$) and thus more robust than using amplitude information alone (equation (S1) and Table S1 in Supporting Information). The application of such an approach in the field was limited in the past, given that the entire raw signal was generally not registered during continuous field measurements but would be needed to compute frequency characteristics.

5. Conclusions

Systematic flume experiments were performed to quantify the effect of particle size, mean water flow velocity, bed roughness and bed load material (particle shape) on the signal registered by the Swiss plate geophone, a bed load surrogate monitoring device. We quantified the effect of these parameters on the impulse counts, a characteristic summary value of the geophone signal that has proven to be the most robust simple metric for measuring bed load transport rates with this system [*Rickenmann et al.*, 2012, 2014]. The impulses per unit mass of transported particles were found to depend strongly on particle-size D, mean flow velocity V_W, and bed roughness, and to a minor extent on bed load material type (particle shape). These observations explain some differences in established impulse bed load mass

calibration coefficients between field sites with direct bed load calibration measurements [*Rickenmann et al.*, 2014].

The flume experiments further revealed that the size of the bed load particles transported over the Swiss plate geophone can be estimated not only from the amplitude, but also from the frequency of the geophone signal. Combining frequency and amplitude information resulted in a more robust identification of the transported particles size D over a wide range of particle sizes than using amplitude information alone.

Using these findings of the flume experiments and a more sophisticated preprocessing of the raw signal (or its complete storage) during field measurements may increase the accuracy of bed load transport measurements with the Swiss plate geophone system in future.

Notation

A	signal amplitude.
A_{FFT}	Fourier amplitude.
$A_{max,P}$	maximum registered amplitude within a packet.
D	particle size.
D_m	mean particle size.
$\Delta_{t,I}$	duration of an impulse.
$\Delta_{t,P}$	duration of a packet.
FFT	fast Fourier transform.
Fr	Froude number.
$f_{centroid}$	centroid frequency.
f_{char}	characteristic frequency.
f_s	sampling rate.
PSD	particle size distribution.
G_m	particle weight.
g	gravitational acceleration.
h_W	water depth.
I	number of impulses.
I_j	number of impulses triggered by particle size class j.
k_b	linear relation coefficient between I and M_{tot}.
k_{bj}	linear relation coefficient between I_j M_{bj}.
M_{bj}	transported bed load mass for particle-size fraction j.
M_{tot}	total transported bed load mass.
NG	number of particles.
P	number of packets.
R	experimental run.
Re	Reynolds number.
R_h	hydraulic radius.
V_W	mean flow velocity.

Acknowledgments
The authors are grateful to numerous WSL and VAW colleagues for their support in the flume experiments. This study was supported by the Swiss National Science Foundation SNSF (grant 200021_137681). Please contact Dieter Rickenmann (dieter.rickenmann@wsl.ch) if you are interested in the data used in this paper. We thank for the feedback of Christophe Ancey (Associate Editor), Jonathan B. Laronne, and two anonymous reviewers which helped to improve the paper.

References

Abd-Elfattah, A., and A. M. Omima (2009), Estimation of the unknown parameters of the generalized Frechet distribution, *J. Appl. Sci. Res.*, *5*(10), 1398–1408.

Ancey, C., F. Bigillon, P. Frey, J. Lanier, and R. Ducret (2002), Saltating motion of a bead in a rapid water stream, *Phys. Rev. E*, *66*(3), Part 2B, 036306, doi:10.1103/PhysRevE.66.036306.

Auel, C., I. Albayrak, and R. M. Boes (2015), Bed-load particle motion in supercritical open channel flow, in *36th IAHR World Congress*, The Hague, Netherlands.

Barrière, J., A. Krein, A. Oth, and R. Schenkluhn (2015), An advanced signal processing technique for deriving grain size information of bed-load transport from impact plate vibration measurements, *Earth Surf. Processes Landforms*, *40*, 913–924, doi:10.1002/esp.3693.

Barton, J. S., R. L. Slingerland, S. Pittman, and T. B. Gabrielson (2010), Monitoring coarse bedload transport with passive acoustic instrumentation: A field study, *U.S. Geol. Surv. Sci. Invest. Rep., 2010-5091*, 38–51.

Belleudy, P., A. Valette, and B. Graff (2010), Passive hydrophone monitoring of bedload in river beds: First trials of signal spectral analyses, *U.S. Geol. Surv. Sci. Invest. Rep., 2010-5091*, 67–84.

Benn, D. I., and C. K. Ballantyne (1993), The description and representation of particle shape, *Earth Surf. Processes Landforms*, *18*(7), 665–672, doi:10.1002/esp.3290180709.

Beylich, A. A., and K. Laute (2014), Combining impact sensor field and laboratory flume measurements with other techniques for studying fluvial bedload transport in steep mountain streams, *Geomorphology*, *218*, 72–87, doi:10.1016/j.geomorph.2013.09.004.
Bogen, J., and K. Møen (2003), Bed load measurements with a new passive acoustic sensor, in *Erosion and Sediment Transport Measurement in Rivers: Trends and Explanation (Proceedings of the Oslo Workshop, June 2002)*, vol. 283, edited by J. Bogen, T. Fergus, and D. E. Walling, pp. 181–182, IAHS Publ. 283, Oslo.
Bunte, K. (1996), Analyses of the temporal variation of coarse bedload transport and its grain size distribution, *Rep. RM-GTR-288*, U.S. Dep. of Agric., Rocky Mt. Res. Stn., Fort Collins, Colo.
Bunte, K., and S. Abt (2001), Sampling surface and subsurface particle-size distributions in wadable gravel- and cobble-bed streams for analyses in sediment transport, hydraulics, and streambed monitoring, *Tech. Rep. RMRS-GTR-74*, Dep. of Agric., For. Serv., Rocky Mt. Res. Stn., Fort Collins, Colo.
Bunte, K., S. R. Abt, J. P. Potyondy, and S. E. Ryan (2004), Measurement of coarse gravel and cobble transport using portable bedload traps, *J. Hydraul. Eng.*, *130*(9), 879–893, doi:10.1061/(ASCE)0733-9429(2004)130:9(879).
Burtin, A., L. Bollinger, J. Vergne, R. Cattin, and J. L. Nábělek (2008), Spectral analysis of seismic noise induced by rivers: A new tool to monitor spatiotemporal changes in stream hydrodynamics, *J. Geophys. Res.*, *113*, B05301, doi:10.1029/2007JB005034.
Burtin, A., R. Cattin, L. Bollinger, J. Bollinger, J. Vergne, P. Steer, A. Robert, N. Findling, and C. Tiberi (2011), Towards the hydrologic and bed load monitoring from high-frequency seismic noise in a braided river: The "torrent de St Pierre," French Alps, *J. Hydrol.*, *408*, 43–53, doi:10.1016/j.jhydrol.2011.07.014.
Camenen, B., M. Jaballah, T. Geay, P. Belleudy, J. Laronne, and J. Laskowsky (2012), Tentative measurements of bedload transport in an energetic alpine river, in *River Flow*, edited by R. Murillo Muñoz, pp. 379–386, CRC Press, San José, Costa Rica.
Einstein, H. A. (1937), Bedload transport as a probability problem, in *Sedimentation*, edited by H. W. Shen, pp. 1–105, Colo. State Univ., Fort Collins.
Emmett, W. W. (1980), A field calibration of the sediment-trapping characteristics of the Helley-Smith bedload sampler, *U.S. Geol. Surv. Prof. Pap.*, *1139*, 44 p.
Esbensen, K. H., P. K. Ade, J. F. Zuta, J. Bogen, and K. Møen (2007), Acoustic chemometrics of complex natural systems: Flume test rig feasibility studies for monitoring river bed-load sediment transportation processes, *J. Chemometrics*, *21*, 459–473, doi:10.1002/cem.1076.
Etter, M. (1996), Zur erfassung des geschiebetransportes mit hydrophonen [Recording bedload transport with hydrophones], PhD thesis, Univ. of Berne, Berne, Switzerland, Swiss Federal Research Institute WSL, Birmensdorf, Switzerland.
Geay, T. (2013), Mesure acoustique passive du transport par charriage dans les rivières [Passive acoustic measurement of bedload transport], PhD thesis, Univ. Joseph Fourrier de Grenoble, Grenoble, France.
Goto, K., T. Itoh, T. Nagayama, M. Kasai, and T. Marutani (2014), Experimental and theoretical tools for estimating bedload transport using a Japanese pipe hydrophone, *Int. J. Erosion Control Eng.*, *7*(4), 101–110.
Gray, J. R., J. B. Laronne, and J. D. G. Marr (2010), Bedload-surrogate monitoring technologies, *U.S. Geol Surv. Sci. Invest. Rep. 2010–5091*, 37 p.
Hager, W. H. (1999), *Wastewater Hydraulics: Theory and Practice*, Springer-Verlag, Berlin, London.
Hegglin, R. (2011), *Beiträge zum Prozessverständnis des fluvialen Geschiebetransports*, diploma thesis, 87 pp., Univ. of Berne and WSL, Birmensdorf, Switzerland.
Helley, E. J., and W. Smith (1971), Development and calibration of a pressure-difference bedload sampler, *U.S. Geol. Surv. Open File Rep., 73-108*, 38 p.
Hu, C., and Y. Hui (1996), Bed-load transport. I: Mechanical characteristics, *J. Hydraul. Eng.*, *122*(5), 245–254.
Hubbell, D. W. (1964), Apparatus and techniques for measuring bedload, *U.S. Geol. Surv. Water Supply Pap.*, *1748*, pp. 74.
Ibbeken, H. (1974), A simple sieving and splitting device for field analysis of coarse grained sediments, *J. Sediment. Petrol.*, *44*, 939–946, doi:10.1306/74D7295F-2B21-11D7-8648000102C1865D.
Krein, A., H. Klinck, M. Eiden, W. Symader, R. Bierl, L. Hoffmann, and L. Pfister (2008), Investigating the transport dynamics and the properties of bedload material with a hydro-acoustic measuring system, *Earth Surf. Processes Landforms*, *33*, 152–163, doi:10.1002/esp.1576.
Lajeunesse, E., L. Malverti, and F. Charru (2010), Bed load transport in turbulent flow at the grain scale: Experiments and modeling, *J. Geophys. Res.*, *115*, F04001, doi:10.1029/2009JF001628.
Mao, L., R. Carrillo, C. Escauriaza, and A. Iroume (2016), Flume and field-based calibration of surrogate sensors for monitoring bedload transport, *Geomorphology*, *253*, 10–21, doi:10.1016/j.geomorph.2015.10.002.
Mason, T., D. Priestley, and D. E. Reeve (2007), Monitoring near-shore shingle transport transport under waves using a passive acoustic technique, *J. Acoust. Soc. Am.*, *122*(2), 737–745, doi:10.1121/1.2747196.
Meyer-Peter, E., and R. Müller (1948), Formulas for bedload transport, paper presented at 2nd Meeting of International Association of Hydraulic Structures Research, Stockholm, Sweden.
Mizuyama, T., et al. (2010a), Calibration of a passive acoustic bedload monitoring system in Japanese mountain rivers, *U.S. Geol. Surv. Sci. Invest. Rep.*, *2010-5091*, 296–318.
Mizuyama, T., A. Oda, J. B. Laronne, M. Nonaka, and M. Matsuoka (2010b), Laboratory tests of a Japanese pipe geophone for continuous acoustic monitoring of coarse bedload, *U.S. Geol. Surv. Sci. Invest. Rep.*, *2010-5091*, 319–335.
Møen, K. M., B. J. Bogen, J. F. Zuta, P. K. Ade, and K. Esbensen (2010), Bedload measurement in rivers using passive acoustic sensors, *U.S. Geol. Surv. Sci. Invest. Rep.*, *2010-5091*, 336–351.
Pecorari, C. (2013), Characterizing particle flow by acoustic emission, *J. Nondestr. Eval.*, *32*(1), 104–111, doi:10.1007/s10921-012-0163-7.
Reid, I., J. T. Layman, and L. E. Frostick (1980), The continuous measurement of bedload discharge, *J. Hydraul. Res.*, *18*(3), 243–249, doi:10.1080/00221688009499550.
Rennie, C. D., and M. Church (2010), Mapping spatial distributions and uncertainty of water and sediment flux in a large gravel bed river reach using an acoustic Doppler current profiler, *J. Geophys. Res.*, *115*, F03035, doi:10.1029/2009JF001556.
Rickenmann, D. (2016), Bedload transport measurements with geophones, hydrophones and underwater microphones (passive acoustic methods), in *Gravel Bed Rivers and Disasters*, edited by D. Tsutsumi and J. B. Laronne, John Wiley, in press.
Rickenmann, D., and B. Fritschi (2010), Bedload transport measurements using piezoelectric impact sensors and geophones, *U.S. Geol. Surv. Sci. Invest. Rep.*, *2010-5091*, 407–423.
Rickenmann, D., J. M. Turowski, B. Fritschi, A. Klaiber, and A. Ludwig (2012), Bedload transport measurements at the Erlenbach stream with geophones and automated basket samplers, *Earth Surf. Processes Landforms*, *37*, 1000–1011, doi:10.1002/esp.3225.
Rickenmann, D., C. R. Wyss, J. M. Turowski, V. Weitbrecht, and R. M. Boes (2014), Geschiebemessungen mit Geophon-sensoren: Ableitung der Kalibrierfunktion durch Messungen im Feld und Labor, in *Internationales Symposium Wasser- und Flussbau im Alpenraum*, edited by R. M. Boes et al., pp. 355–365, Versuchsanstalt für Wasserbau, Hydrologie und Glaziologie, ETH Zürich, Zürich.

Roth, D. L., E. E. Brodsky, N. J. Finnegan, J. M. Turowski, A. Badoux, and D. Rickenmann (2015), Sediment transport inferred from seismic signals near a river, *J. Geophys. Res. Earth Surf.*, *121*, 725–747.

Schwalt, M., and W. Hager (1992), Die Strahlbox (The jet-box), *Schweizer Ingenieur und Architekt*, *100*(27/28), 547–549.

Shields, A. (1936), Anwendung der Aehnlichkeitsmechanik und der Turbulenzforschung auf die Geschiebebewegung, technical report 26, Mitteilungen der Preussischen Versuchsanstalt für Wasserbau und Schiffbau, Berlin.

Sneed, E. D., and R. L. Follk (1958), Pebbles in the Lower Colorado River, Texas: A study in particle morphogenesis, *J. Geol.*, *66*(2), 114–150.

Taniguchi, S., Y. Itakura, K. Miyamoto, and J. Kurihara (1992), A new acoustic sensor for sediment discharge measurements, in *Erosion and Sediment Transport Monitoring Programmes in River Basins*, vol. 210, pp. 135–142, IAHS Publ., Oslo.

Thorne, P. D. (1986), Laboratory and marine measurements on the acoustic detection of sediment transport, *J. Acoust. Soc. Am.*, *80*(3), 899–910.

Thorne, P. D. (2014), An overview of underwater sound generated by interparticle collisions and its application to the measurements of coarse sediment bedload transport, *Earth Surf. Dyn.*, *2*, 531–543, doi:10.5194/esurf-2-531-2014.

Tsakiris, A. G., A. N. Papanicolaou, and T. Lauth (2014), Signature of bedload particle transport mode in the acoustic signal of a geophone, *J. Hydraul. Res.*, *52*(2), 185–204, doi:10.1080/00221686.2013.876454.

Turowski, J. M., and D. Rickenmann (2009), Tools and cover effects in bedload transport observations in the Pitzbach, Austria, *Earth Surf. Processes Landforms*, *34*, 26–37, doi:10.1002/esp.1686.

Turowski, J. M., M. Böckli, D. Rickenmann, and A. Beer (2013), Field measurements of the energy delivered to the channel bed by moving bed load and links to bedrock erosion, *J. Geophys. Res. Earth Surf.*, *118*, 2438–2450, doi:10.1002/2013JF002765.

Turowski, J. M., C. R. Wyss, and A. R. Beer (2015), Grain size effects on energy delivery to the stream bed and links to bedrock erosion, *Geophys. Res. Lett.*, *42*, 1775–1780, doi:10.1002/2015GL063159.

Uher, M., and P. Benes (2012), Measurement of particle size distribution by acoustic emission method, paper presented at XX IMEKO World Congress, Busan, South Korea.

Wyss, C. R., D. Rickenmann, B. Fritschi, J. M. Turowski, V. Weitbrecht, and R. M. Boes (2016a), Measuring bedload transport rates by grain-size fraction using the Swiss plate geophone at the Erlenbach, *J. Hydraul. Eng.*, 1–11, doi:10.1061/(ASCE)HY.1943-7900.0001090.

Wyss, C. R., D. Rickenmann, B. Fritschi, J. M. Turowski, V. Weitbrecht, E. Travaglini, E. Bardou, and R. M. Boes (2016b), Laboratory flume experiments with the Swiss plate geophone bedload monitoring system: 2. Application to field sites with direct bedload samples, *Water Resour. Res.*, *52*, doi:10.1002/2016WR019283.